



# Fatigue crack growth modeling of pipeline steels in high pressure gaseous hydrogen<sup>☆</sup>



Robert L. Amaro, Elizabeth S. Drexler, Andrew J. Slifka<sup>\*</sup>

Applied Chemicals and Materials Division, Materials Measurement Laboratory, National Institute of Standards and Technology, 325 Broadway, Boulder, CO 80305, USA

## ARTICLE INFO

### Article history:

Received 1 November 2012  
Received in revised form 16 April 2013  
Accepted 10 October 2013  
Available online 21 October 2013

### Keywords:

Hydrogen-assisted fatigue crack growth  
High-pressure hydrogen  
Fatigue crack growth modeling

## ABSTRACT

Hydrogen will likely play a key role in a future clean energy economy. However, fundamental understanding of the deleterious effects of hydrogen on the fatigue and fracture properties of pipeline steels is lacking. Furthermore, engineering tools for design and lifetime prediction of pipeline steels in gaseous hydrogen are yet to be developed and implemented into national codes. A constitutive model that couples deformation and hydrogen-diffusion, supporting a phenomenological predictive model for fatigue crack growth, is presented for pipeline steels in high-pressure gaseous hydrogen. The semi-empirical model is predicated upon the hypothesis that one of two mechanisms dominates the fatigue crack growth response, depending upon the applied load and the material's hydrogen concentration. The model correlates test results well, and illustrates how the deformation mechanisms contribute to fatigue crack propagation in pipeline steels in environments similar to those found in-service.

Published by Elsevier Ltd.

## 1. Introduction

Hydrogen has been envisioned as a key component to a future sustainable energy infrastructure. General Motors, Ford, Toyota, Honda and Daimler have all indicated that they will have a hydrogen fuel cell vehicle in production by 2015. However, the current gaseous hydrogen transportation infrastructure in the United States is nowhere near sufficient to support nation-wide sales of hydrogen fuel cell vehicles. Current gaseous hydrogen transportation schemes include hydrogen-specific tube trailers via highway or rail, and pipelines. Hydrogen transport via tube trailer is highly inefficient and insufficient to meet the envisioned demand. Hydrogen transport via steel pipelines is the most cost efficient method to transport hydrogen across the nation [1]. Given that hydrogen has deleterious effects upon steel deformation and fatigue response [2], a full understanding of the constitutive behavior of pipeline steels exposed to gaseous hydrogen is necessary prior to the introduction of hydrogen in pipelines. Furthermore, predictive models that account for the pipeline constitutive behavior and fatigue response are required. Finally, national codes and standards that incorporate the state of the art understanding of hydrogen's effect upon pipeline steels, including predictive measures for deformation and fatigue, must be created. This work describes a simple constitutive model, coupled with an existing fatigue crack

growth rate (FCGR) predictive model, which has been implemented in MATLAB.<sup>1</sup> The coupled constitutive-FCG model has been calibrated to two API pipeline steels [3]. Calibration was performed by use of monotonic tensile test results in high pressure gaseous hydrogen as well as FCG tests performed on compact tension (CT) specimens in high pressure gaseous hydrogen. Model predictive efficacy to CT specimen tests is provided. The model is then implemented in conjunction with a stress intensity factor solution in closed-form to predict FCGR in pipes having internal thumbnail shaped cracks. Model predictive capabilities for pipe geometry are discussed in reference to literature results on pressure vessels of similar geometry.

## 2. Materials

Monotonic tension and constant load FCG tests were performed on API-5L X52 and X100 pipeline steels. The nominal chemical composition of the materials tested is provided in Table 1 and optical micrographs of the microstructures are provided in Fig. 1.

The X52 microstructure had a characteristic length scale of approximately 10  $\mu\text{m}$  and was composed of ferrite and pearlite. The X100 microstructure had a characteristic length scale on the

<sup>☆</sup> Contribution of NIST, an agency of the US government; not subject to copyright.

<sup>\*</sup> Corresponding author. Tel.: +1 303 497 3744; fax: +1 303 497 5030.

E-mail address: [slifka@boulder.nist.gov](mailto:slifka@boulder.nist.gov) (A.J. Slifka).

<sup>1</sup> Commercial equipment, instruments, or materials are identified only in order to adequately specify certain procedures. In no case does such identification imply recommendation or endorsement by the National Institute of Standards and Technology, nor does it imply that the products identified are necessarily the best available for the purpose.

**Table 1**  
Nominal chemical composition (wt%) for alloys tested.

	C	Mn	Si	S	P	Ni	Cr	Mo	Nb + V + Ti	Fe
X100	0.064	1.870	0.099	<0.001	0.009	0.470	0.023	0.230	0.036	Bal
X52	0.060	0.087	0.120	0.006	0.011	0.020	0.030	–	0.036	Bal

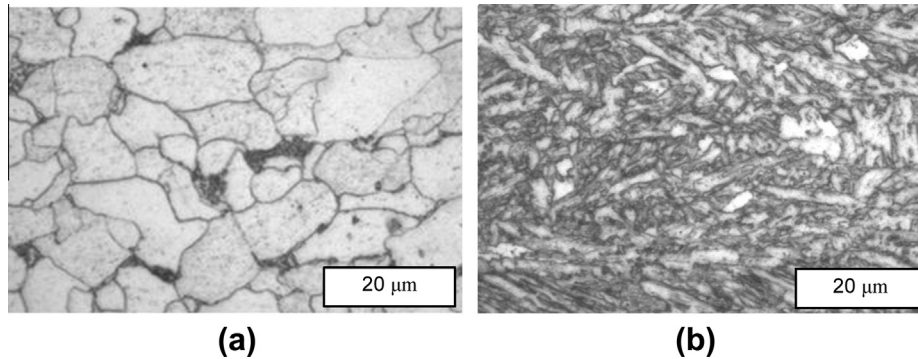


**Fig. 1.** Optical micrographs of (a) X52 and (b) X100 microstructures [4].

order of 1  $\mu\text{m}$  and was composed primarily of bainite and acicular ferrite [4].

### 3. Experimental procedure

Round tensile specimens were machined from late 1990s vintage X52 and X100 pipeline steels per ASTM E8/E8M [5]. Monotonic displacement-controlled tensile tests were performed on an MTS 100 kN servo hydraulic load frame equipped with control software from the manufacturer. All tests were performed in a stainless steel pressure vessel (regardless of environment) rated to 138 MPa internal pressure. Strain was measured by use of an extensometer having 25.4 mm gage length, 38 mm range and a resolution of 1  $\mu\text{m}$ . Force was measured by use of a load cell of proving ring design. The load cell was located inside of the pressure vessel in series with the test specimen and hydraulic actuator. The load cell has a capacity of 10 kip (44 kN) and a resolution of 5 lbf (0.02 kN). Hydrogen used during tensile testing was generated by an on-site electrolyzer. Test results of hydrogen purity are provided in [4]. Monotonic tensile test results are provided in [4].

Load-controlled fatigue crack growth experiments were performed on the same API-5L pipeline steels discussed above. Compact tension specimens in the transverse-longitudinal orientation were tested on a closed-loop 22 kip (100 kN) servo-hydraulic load frame. Tests performed in high-pressure hydrogen (250 psi (1.72 MPa), 1000 psi (6.89 MPa), 3000 psi (20.68 MPa) and 7000 psi (48.26 MPa)) were conducted in a 20 ksi (138 MPa) pressure vessel. Test control was handled by the MTS Multi-Purpose Testware software with built-in load control functionality. All tests were performed per ASTM E647-08 [6]. Feedback for the force loop was provided by a 10 kip (44 kN) proving ring located inside the pressure vessel. The proving ring had a 5 lbf (0.02 kN) resolution. Crack mouth opening displacement was monitored via a clip gage having a 3 mm range and 0.001 mm resolution. Hydrogen gas was either electrolyzed from ultrapure water or provided in “commercially pure” form (99.9999%  $\text{H}_2$ ) from an outside vendor. Hydrogen purity was tested periodically by an outside vendor. Hydrogen pressure was maintained during testing via a program written in-house using LabVIEW. All test results reported here were conducted at a load ratio of  $R_f = 0.5$  and a frequency of 1 Hz. The X100 specimens tested were all machined from the same section of pipe, i.e., the same heat, as was the case for the X52 specimens.

### 4. Test results

Monotonic test results of API-5L X52 and X100 pipeline steels in high pressure gaseous hydrogen are shown as a function of hydrogen pressure in Fig. 2 [4]. The modeling here requires the use of true stress–strain relationships. As such the engineering stress–strain data from [4], and shown in Fig. 2, was converted to true stress–strain data up to the point of necking. The true stress–strain response up to 20% strain is shown in Fig. 3.

In general, the presence of hydrogen considerably decreases the ductility of the material, as can be seen by the differences in elongation at failure for the specimens tested in air versus hydrogen (Fig. 2). Furthermore, hydrogen appears to have a minimal impact on the strain at which necking occurs.

Fatigue crack growth test results in air and high pressure hydrogen are provided in Fig. 4.

The FCGR results indicate that the hydrogen-assisted (HA) FCG response approaches that of the air response, at combinations of low hydrogen pressures and low  $\Delta K$ . That is, the results indicate that at low hydrogen pressure and sufficiently low  $\Delta K$ , the HA FCG would match the FCG response in air. Suresh and Ritchie [7] characterized the transition point at which the HA FCG deviates from that of air as  $K_{max}^T$ , or the transition cycle maximum stress intensity factor. Furthermore, the results indicate that the HA FCG increases with increasing hydrogen test pressure for values of  $\Delta K$  below about 20 MPa  $\text{m}^{1/2}$ . Above this value, the HA FCG trends tend to converge, regardless of hydrogen pressure. Finally, there exists a transition point in the HA FCG data at approximately  $\Delta K_{tr} \sim 13.0 \text{ MPa} \cdot \text{m}^{1/2}$ , corresponding to a fatigue crack growth per cycle of  $da/dN_{tr} \sim 3 \times 10^{-4} \text{ mm/cycle}$ . The HA FCG occurring below this transition ( $da/dN < da/dN_{tr}$ ) will be referred to as “transient” HA FCG. Hydrogen-assisted FCG occurring above the transition ( $da/dN > da/dN_{tr}$ ) will be referred to as “steady state” HA FCG, for the remainder of this work. The experimental results indicate that  $da/dN_{tr}$  occurs at

$$da/dN_{tr} = 2 \times 10^{-6} \Delta K^2 \quad (1)$$

for both materials tested. The results of Eq. (1) are identical to the second-order estimate of the Irwin plastic zone size for X100 and are proportional to the plastic zone size for X52. It is hypothesized that the transient HA FCG results from crack extension per cycle on the order of (or smaller than) the region of highest hydrostatic

Download English Version:

<https://daneshyari.com/en/article/7172349>

Download Persian Version:

<https://daneshyari.com/article/7172349>

[Daneshyari.com](https://daneshyari.com)